Tree Physiology 39, 156–165
doi:10.1093/treephys/tpy051

Methods paper

Do nano-particles cause recalcitrant vulnerability curves in *Robinia*? Testing with a four-cuvette Cochard rotor and with water extraction curves

Guangyuan Du[1,2], Feng Feng[2,5], Yujie Wang [3] and Melvin T. Tyree[2,4]

[1]College of Science, Northwest A&F University, Yangling 712100, Shaanxi, China; [2]College of Forestry, Northwest A&F University, Yangling 712100, Shaanxi, China; [3]Biology Department, University of Utah, Salt Lake City, UT 84112, USA; [4]College of Chemistry and Life Sciences, Zhejiang Normal University, Jinhua 321004, Zhejiang, China; [5]Corresponding author (fengfeng12343@126.com)

Received November 29, 2017; accepted May 3, 2018; published online May 19, 2018; handling Editor Frederick Meinzer

Cavitation resistance is a key trait for characterizing the drought adaption in plants and is usually presented in terms of vulnerability curves. Three principal techniques have been developed to produce vulnerability curves, but curves generated with centrifugation are reported to suffer from artifacts when applied to long-vesseled species. The main cause of this artifact is the issue of open vessels, resulting in a nano-particle effect that may seed premature embolism. We used two methods to test the potential mechanism behind the nano-particle effect in centrifuge-based vulnerability curves. A four-cuvette rotor system based on a traditional Cochard rotor was designed to inhibit effervescence while injecting water, but the recalcitrant vulnerability curves in *Robinia* could not be eliminated. There may be multiple sources, besides effervescence, of hypothetical nano-particles: they may arise from cut surfaces or they may be always present in the injected water, leading to the premature embolisms. To prevent the entry of the hypothetical nano-particles, water extraction curves in terms of PLV (percentage loss volume of extracted water from stems) vs tensions were constructed. The PLV curves of *Robinia* showed s-shaped characteristics after subtracting the first Weibull components from water extraction curves, which were not related to the water loss from vessels according to dye staining experiments. The differences between T_{50} (xylem tension at which 50% of hydraulic conductivity is lost) in mean PLV curve and T_{50} in percentage loss of conductivity curves determined by the four-cuvette rotor system and by the bench dehydration method were 3.9 MPa and 0.7 MPa, respectively. Hence, PLV curves may be a valid way to measure the cavitation resistance in long-vesseled species with centrifugation. Keeping bark intact in the process of measurement is recommended, otherwise it would increase evaporation from the entire system.

Keywords: extraction, flow rotor, micro-bubbles, open vessel artifact, water deficit.

Introduction

Hydraulic failure is now widely recognized as a common mechanism for drought-induced mortality in woody plants (Tyree and Sperry 1989, McDowell et al. 2008), which has implications for forest dieback (Breshears et al. 2005, Allen et al. 2010) and climate change (Allison et al. 2009, Choat 2013). As the soil dries, a cavitation event occurs when sufficient tension develops in the xylem, which breaks the continuous water column. The result of cavitation is an embolized conduit in which water has been displaced by water vapor and/or air, reducing the capacity of the plant to move water to the canopy. In the present context, the terms cavitation and embolism are practically synonymous because of their causal association. Then, the plant will desiccate and die if the drought condition does not ease before complete hydraulic failure occurs. The resistance of a plant to cavitation is a key trait in characterizing the adaption to drought. This is usually presented in terms of P_{50} or T_{50}, the xylem pressure (negative value) or tension (positive value) at which 50% of hydraulic

conductivity is lost. Note that pressure and tension are usually measured relative to atmospheric pressure. Hence, absolute negative pressure and true tension occurs at about −0.1 MPa, which equals the atmospheric pressure at true zero gas pressure.

The value of T_{50} is calculated from a vulnerability curve (VC), which plots the percentage loss of hydraulic conductivity (PLC) in stems as a function of tension. Two types or shapes of vulnerability curves are common: they are either r-shaped (exponential) curves or s-shaped (sigmoid) curves. Three major methods have been used to determine vulnerability curves for over 1200 species. If these curves are going to be used to interpret climate change issues or for other eco-physiological studies, it is imperative that all methods give the same results. Unfortunately, there are a growing number of instances in which the three major methods give very different VCs for the same species (Wang et al. 2014*a*). The three different methods have been unified in past research by the concept that air-seeding across pit membranes cause embolisms, and thus loss of hydraulic conductivity, over the entire VC. Since the three techniques give very different results, it is necessary to ask why. Are the VCs different because the different techniques produce embolisms by different mechanisms? If so, which technique best simulated the mechanisms involved in the whole plants growing in their ecosystems? Our lab has been working on a series of papers to examine what the mechanisms are in each method. The 'gold standard' is assumed to be the bench dehydration method, wherein excised shoots, which are cut longer than the longest vessels, are dehydrated in a controlled lab environment while measuring xylem tension and harvesting stem segments to monitor the loss of hydraulic conductivity (K_h) to construct a VC. The other methods are the air-injection or pressure sleeve method and the centrifuge method.

In this paper, we focus on recent advances of understanding the mechanisms of anomalous cavitation observed in the same plants that have 'recalcitrant' VCs when measured in a centrifuge (Choat et al. 2010, Cochard et al. 2013, Martin-StPaul et al. 2014). Recalcitrant curves are r-shaped and have T_{50} values that are too low and are thus inconsistent with the known water relations of the species. Wang et al. (2014*a*) demonstrated that *Robinia pseudoacacia* stems, which showed the recalcitrant curves, had vessel lengths that were greater than or equal to half the length of the stem segment spinning in the centrifuge. In addition Wang et al. (2014*a*) obtained results that supported the hypothesis that premature cavitation occurred at an overly low tension, when nano-particles were drawn into the vessels from the cuvettes in the centrifuge. Nano-particles could be nano-bubbles, nano-solids and impurities in the water including ions, acting as nuclei to induce cavitation. If vessels were very short, the pit membranes between vessels would filter out these hypothetical particles before they reached the axis of rotation where the pressure was most negative. This hypothesis could partly explain why long-vessel species have r-shaped curves and short-vessel species do not. However the hypothesis is useful only if we can amass more data consistent with the hypothesis. Centrifugation is the most efficient method to simulate tension in excised shoots in laboratory, but it should not be broadly accepted in long-vessel species studies until reasons for the 'artificial' r-shaped VCs are examined. One way is to redesign the rotor to eliminate the number of particles entering the vessels from the cuvettes and show that recalcitrant species have more reasonable VCs than they do before the redesign. The other way is to try alternative centrifuge-based strategies for measuring VCs in such a way that the hypothetical particles cannot enter the vessels, such as avoiding the injection procedure and looking for other cavitation-related parameters instead of 'volume extraction' (see details below).

The rotor redesign that we tested was intended to remove just one of several possible sources of particles that might seed premature embolisms. The nano-particles might arise in three different ways: they might be generated at the recently cut surfaces of stem cross sections, they might always be present in the injected water or they might be generated by the water injection process. Figure 1a shows how water is injected through a fill tube. The water is accelerated by the centrifuge to strike the water surface in a cuvette at high speed and with sufficient force to cause

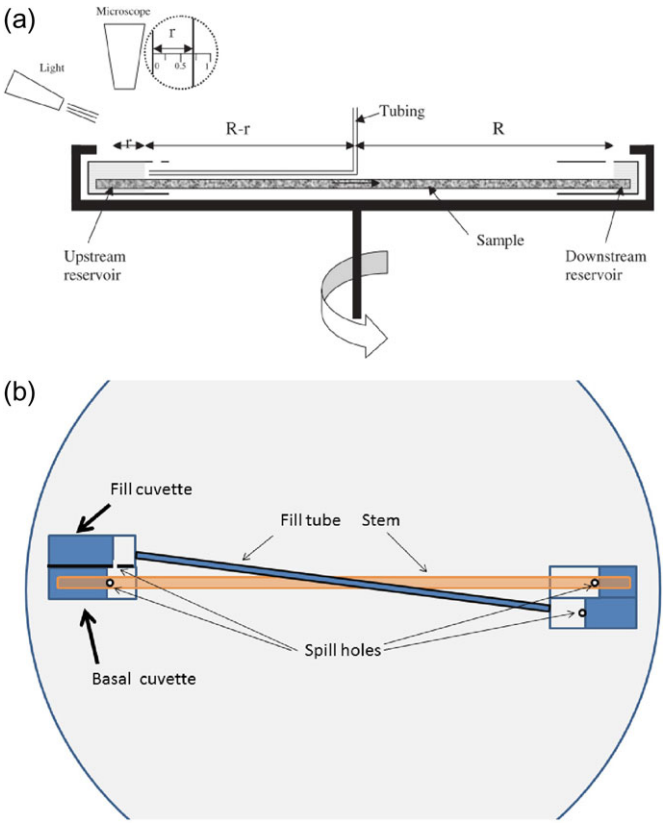

Figure 1. (a) The schematic drawing of the Cochard rotor (Cochard 2002). (b) Top view of the four-cuvette rotor system. The rotor system has room for a stem of 27.3 cm in length and ~0.7 cm in diameter. See Wang et al. (2014*b*) for more mechanical details and theory of measurement.

effervescence. This idea was tested experimentally by Wang et al. (2014*a*), who continuously measured the K_h over 4 h at a constant low tension of 0.031 MPa which caused variable declines in K_h. The magnitude of the decline was correlated with the vessel length; hence, the gradual loss of K_h with time might have been caused by nano-particles. A four-cuvette rotor (Figure 1b) was subsequently built and developed based on the Cochard rotor because we believed the above problem could be reduced or prevented by physically separating the cuvette that receives the injection (where effervescence occurs) from the cuvette needed to measure the flow, except for a small hole for water transmission between adjacent cuvettes. The results will reveal that the four-cuvette system did not eliminate the recalcitrant VCs.

While constructing and testing our new four-cuvette rotor, the Bordeaux lab had used a method to measure VCs that would prevent the entry of hypothetical nano-particles (Pivovaroff et al. 2016). This method was used earlier by Cochard et al. (2010*a*) to detect the effect of the sap ionic concentration on the vulnerability to cavitation. Traditional VCs are based on plots of K_h or percent loss conductivity, PLC = 1 − K_h/K_{max} vs the tension causing the loss of K_h below the maximum initial value, K_{max}. Instead, Cochard et al. (2010*a*) and Pivovaroff et al. (2016) measured percentage loss volume (PLV) of the extracted water from stems. The water was lost by centrifugal extraction of water volume. This process has the advantage of preventing the entry of nano-particles into vessels, because the direction of water flow during extraction is from the axis of rotation to the cuvettes. We used this extraction method on flushed, unflushed, peeled and painted samples of our recalcitrant species, *Robinia*, to test the nano-particle hypothesis. In the test, the PLV of water was calculated using two methods. One method was scaled to the stem volume in order to investigate the contribution of vessel water storage in the stems and the percentage of the volume of the stem. Water storage may be associated with volume changes in living cells of the bark or xylem, e.g., ray cells or xylem parenchyma, which are drained through vessels. The other may be associated with the volume extracted by the cavitation-draining of vessels, which can be detected by staining, whereas the former will not change vessel staining patterns. The second method was scaled to the maximum extracted water from the stem in order to understand the differences between PLV and PLC that were generated by the Cochard rotor. Flushed and unflushed samples were compared to investigate the impact of native embolized vessels on curves constructed by the extraction method. Peeled samples and barkless segments with the radial edge of wood surfaces sealed with paint were used to determine whether the water stored in bark would influence the curves constructed by the extraction method as stated by Pivovaroff et al. (2016) and to determine the role of the bark in preventing evaporation in the measurements. In addition, a camera system was used in recording meniscus movements during centrifugal measurements to identify the occurrence of evaporation during spinning.

Materials and methods

Plant material

Experiments were performed from July to November in 2014 and from October to November in 2016 on *Robinia pseudoacacia* L. growing near the Weihe River in Yangling, Shaanxi, China (34°16′N, 108°4′E, 457 m altitude) and ~3 m above the floodplain. Current-year stems with length of 150–200 cm were collected at dawn or in the evening. The leaves and apices of the sampled stems were removed while submerged in the water of a plastic reservoir after harvesting to eliminate any possible embolisms introduced by excision. The resulting segments were ~40 cm long and the basal diameters were between 5 and 7 mm. All collected branches were stored in the water reservoir during transportation to the laboratory either for centrifugal measurements or for microscopic observation. If the sampled branches were kept overnight before measurements, they were stored in water at 4 °C in a refrigerator.

A four-cuvette rotor

The four-cuvette rotor was fabricated by Hunan Xiang Yi Laboratory Instrument Development Co., Ltd and was specifically fitted to a Xiang Yi H2100R centrifuge (Figure 1b). There was a 5 × 2.5 cm^2 slot at each end of the redesigned rotor where two cuvettes were symmetrically placed side-by-side. There were two cuvettes that received the injection water; one was at the distal end of the rotor, and the other at the basal end of the rotor, and both cuvettes had a spill hole 16 mm from the base of the cuvette, which was necessary for maintaining the balance of the rotor. At the basal end, the spill hole allowed water to flow into the cuvette holding the basal end of the stem segment. The basal cuvette holding the stem had two holes: one was labeled the 'spill hole', which connects the two cuvettes glued together with epoxy, and the other spill hole was 14 mm from the base of the cuvette holding the stem. The maximum meniscus level of the basal cuvette was determined by the 14-mm-high spill hole when water was injected. The fill cuvette receiving the injection effervesced, but because the hole in the fill cuvette is only 2 mm above the meniscus level of the basal cuvette, the water could transfer over to the adjacent cuvette with little effervescence. The two cuvettes on the other side were not cemented, but the cuvette with the distal end of the stem had a spill hole 10 mm from the base. The pressure difference between the cuvettes was computed from $\Delta P = 0.5\rho\omega^2\,[R^2 - (R-r)^2]$, where ρ is the density of water, ω is the angular velocity of the rotor, R is the distance to the low water level and r is the difference in level of the two reservoirs. As water flowed through the stem after the injection, the height difference was reduced from 4 mm to zero because of water flow through the stem.

Vulnerability curves measurements

Branches were trimmed to 27.3 cm long under water with a new razor blade. To avoid air entry into large vessels, stems were kept horizontal whenever they were removed from the water bath and connected to the apparatus. Stem segments were flushed with degassed 0.01 M KCl solution under 150 kPa pressure for 5 min to remove any native embolisms, and the solution was prepared as previously described (Feng et al. 2015). In brief, freshly filtered water was produced by an ultrapure water system (model GYJ 1-10L-S, Huachuang Inc., Chongqing, China) each morning, reagent-grade KCl was added, and then, the solution was stored in a stainless-steel captive air tank (model 3400-002, SHURflo Inc., Cypress, CA, USA) following a 20-min vacuum degassing period. Immediately after flushing, both ends of the segment were respectively placed into the distal and basal cuvettes following filling up the four cuvettes with 0.01 M KCl to the hole level. Details of vulnerability curve measurements and curve fittings were described in Wang et al. (2014*b*), but herein, the two-cuvette rotor and four-cuvette rotor were used, respectively.

Briefly, a difference in the water levels of the cuvettes generates a pressure difference over the branch while spinning; this pressure difference allows the water to run through the segment. Calculation of the conductivity (K_h) in the segment at a given RPM could be achieved by using a standard regression method (Wang et al. 2014*b*). A vulnerability curve was then obtained through stepwise increases in the spinning rate of the centrifuge, subjecting the water in the conduits to increasingly negative xylem pressures, until the percentage loss of conductivity (PLC) reached >95%.

$$\mathrm{PLC} = 100\left(1 - \frac{K_h}{K_{max}}\right) \quad (1)$$

where K_{max} is the maximum conductivity measured in the centrifuge at speed of 1000 RPM after flushing.

A vulnerability curve of the plot of PLC vs either the pressure (negative value) or tension (positive value) was fitted to a single Weibull curve (Eq. 2A) or a dual Weibull curve (Eq. 2B):

$$\mathrm{PLC}/100 = 1 - exp[-(T/B)^C] \quad (2A)$$

$$\mathrm{PLC}/100 = \alpha(1 - exp[-(T/B_1)^{C_1}]) + (1-\alpha)(1 - exp[-(T/B_2)^{C_2}]) \quad (2B)$$

Calibration for menisci position

During water extraction curve measurement, it is essential to make an accurate determination of the water volume in cuvettes while spinning. Calibration error may occur during the measurement because of leakage, evaporation, rotor deviation or cuvette deformation. To achieve this purpose, the position change of menisci with increasing and decreasing RPMs was examined when only two cuvettes with constant water volume were used in the centrifuge (without any branches). A given volume of 0.01 M KCl solution, from 500 to 900 µl was added to each cuvette separately. The volume difference between the 'distal' and 'basal' cuvettes was set to 100, 200, 300 and 400 µl. The top of the two cuvettes were sealed with paraffin film (Parafilm@M) to reduce evaporation during spinning. Subsequently, the cuvettes without stems were mounted in the two sides of the rotor and spun from 600 to 9400 RPM. Cuvettes were weighed before and after spinning to examine if there was any leakage or if significant evaporation occurred. The meniscus position changes vs increasing RPM were fitted to a linear function or a power function by using Matlab cftool, depending on which one best fit the meniscus position. This function was used to correct the menisci positions in the water extraction curve measurements. These tests were conducted on two types of centrifuges, namely, 'CaviTron' (developed by Mel Tyree using an Allegra X-22R, Beckman Coulter at the University of Vermont machine shop) and 'ChinaTron' (developed by Mel Tyree using a model H2100R centrifuge in cooperation with Xiang Yi Lab Instr. Co., Ltd).

Water extraction curve measurements (the Bordeaux method and modifications)

Water extraction curves were examined using flushed samples and unflushed segments to investigate how native embolized vessels contribute to modifying the water extraction curve; water extraction curves were also examined using peeled segments to determine the contribution of water storage in the bark, as well as using barkless segments with the cylindrical of stem surfaces sealed with paint (nail polish).

A water extraction curve quantifies the amount of water that comes out from the stem segment induced at varying tensions while spinning in the centrifuge. Intact cuvettes were used instead of drilled cuvettes. A volume of 600 µl 0.01 M KCl solution needed to be added to each cuvette before spinning. Measurements started at 600 RPM, which is far less than what could induce cavitation in *Robinia* vessels. The menisci in each cuvette were initially unequal because of the unequal water displacement by the unequal apex and basal diameters of the stem segments. The menisci stopped moving and appeared as one within 20 min. The position of this overlapping meniscus was recorded based on a scale in an ocular micrometer. As the speed of the centrifuge increased in a stepwise fashion (0.1, 0.6, 1.1, 1.6, 2.1, 2.6, …, 7.1, 7.6 MPa), the meniscus moved towards the axis of rotation because water flowed out of the stem segment. The RPM was not increased until a small decline in the volume of extracted water was observed through a change in the position of the meniscus in the opposite direction, which was caused by residual evaporation from the stem surface or the cuvette water. The position of the meniscus was recorded at each applied RPM until 9400 RPM, which resulted in a tension of 7.6 MPa at the center of the stem segment. The stem segment was left spinning in the centrifuge for 10–30 min, depending on

the speed. The above technique was essentially similar to that used by the Bordeaux group (Pivovaroff et al. 2016).

After spinning, the areas of both ends of the segment, S_{base} and S_{distal}, were calculated by assuming the stem cross sections had elliptical geometry. The major and minor axes of the cross section were both measured. The water extraction volume, V_e, was calculated by

$$V_e = x_{base,c} \times (S_0 - S_{base}) + x_{distal,c} \times (S_0 - S_{distal}) \quad (3)$$

where $x_{base,c}$ and $x_{distal,c}$ were the corrected basal and distal meniscus positions, respectively. S_0 was the cross area of the cuvette, which was 1 cm^2.

Some measurements were also done with a digital camera system, which controlled the image acquisition from a digital camera (Scout Sc640gm, Basler AG, Germany) with a C-mount lens (HF16 HA-1B, Fujinon Corp., Saitama, Japan). The software recorded centrifuge data (temperature and RPM), calculated the water tension at the axis of rotation, provided the pixel position of the meniscus vs time and saved all relevant data to a text file on a hard disk.

The Archimedes principle was used to measure the volume of the segment, V_{stem}, which could be calculated by the difference between the weights before and after the segment was immersed in a 250 ml cylinder with water and divided by the water density. The relative water extraction volume could be obtained by V_e/V_{stem}. We also calculated the percentage loss volume, PLV = V_e/V_{max} Weibull functions to fit PLV vs tension curves, where V_{max} was the maximum volume of water extracted from the stem segment.

Microscopic observations and staining

A staining method was used to visualize the vessels that embolized in the water extraction experiments above. Preparations for the stem segments were the same as those for the VC measurements and water extraction experiments. The RPM was set to 3363, 4756, 5824, 6725, 7519 RPM, and the corresponding tension induced in the center of the segment was 1, 2, 3, 4, 5 MPa, respectively. After 0.5 h spinning at a given tension, a 4-cm-long segment was cut under water from the center of the spin-treated stem and was subsequently divided into two 2 cm segments for staining.

A gravimetric method was employed for staining through adjusting the height of the glass bottle of dyeing solution, which was placed on a lifting platform. The dyeing solution could only pass through the functional (water-filled) vessels under the force of gravity if the applying pressure and dyeing time were both set properly. Two controls were set up: one used 2-cm-long segments with no embolisms by flushing with 0.01 M KCl at 150 kPa for 2 min; the other used 2-cm-long segments that were fully embolized by air injection at 150 kPa for 2 min. The segments were perfused with 0.02% (w/v) dyeing solution (basic fuchsin + 0.01 m KCl) at a pressure of 0.4 kPa (by setting the height of solution surface at 4 cm) for 1 h, which was determined to be the optimal condition after testing experiments. Then, segments were flushed with 0.01 M KCl at 130 kPa for 5 min to remove excess stain.

A microtome (Leica RM 2235, Nussloch, Germany) was used to cut 18-μm-thick cross sections from the middle of the 2 cm segments. Then, the sections were respectively washed in graded ethanol (35%, 50%, 75% and 95%) for ≥4 s for dehydration and mounted in glycerin on glass slides. Cross sections were photographed under a microscope (Zeiss, Imager A2, Göttingen, Germany) at 50× magnification with a digital camera (Infinity1-5C, Lumenera Corporation, Ottawa, Canada). The camera settings were adjusted to yield optimal image quality using Infinity Capture Application (Version 6.0.0, Lumenera Corporation).

Cross section areas (A) of unstained (embolized) and stained (functional) conduits were measured with WinCell Pro version 2012a (Regent Instruments Inc., Quebec City, Canada). Equivalent radii (r) were determined by $r = (A/\pi)^{1/2}$. According to the Hagen–Poiseuille law, the volume flux of a vessel is linearly proportional to r^4, and therefore the theoretical PLC based on stained results can be obtained by

$$PLC_{stain},\ \% = \frac{\sum_{unstained} r^4}{\sum_{unstained+stained} r^4} \times 100 \quad (4)$$

Results

Vulnerability curves measured by the four-cuvette rotor

The phenomenon of effervescence in the basal cuvette may have been suppressed in the four-cuvette system, since the meniscus sometimes disappeared in the traditional two-cuvette system when water was injected, but this seldom occurred in the four-cuvette system. Compared with the VCs measured by the bench-top dehydration method, a four-cuvette rotor still produced r-shaped VCs with T_{50} = 0.70 ± 0.07 MPa (Figure 2). The VCs generated by the four-cuvette system were significantly less vulnerable than those of the two-cuvette system, until the tension exceeded 1.4 MPa ($P < 0.05$). In a further attempt to suppress nano-bubbles caused by injection-induced effervescence, we filled the injection cuvettes (Figure 1b) with cotton fiber, but this made no difference to the r-shaped curves or the T_{50} value (data not shown).

Calibration for menisci positions

In the branchless water-filled cuvette spinning trials, the evaporation was minimal because the cuvettes were sealed with paraffin film. During ~1 h of spinning, the water weight differences in cuvettes measured by a digital balance were less than 0.001 g.

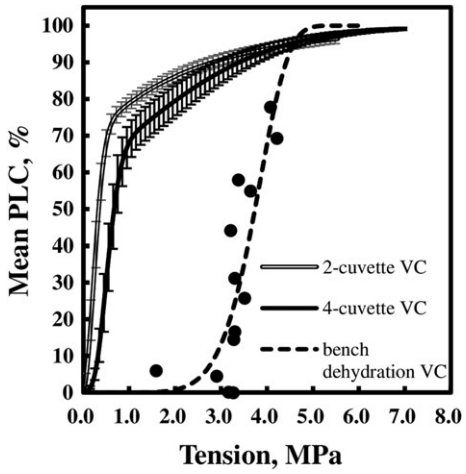

Figure 2. The VCs obtained on two- and four-cuvette rotor where water injections were made to cuvettes shown in Figure 1. The VCs obtained by bench dehydration methods are reproduced from Wang et al. (2014*a*).

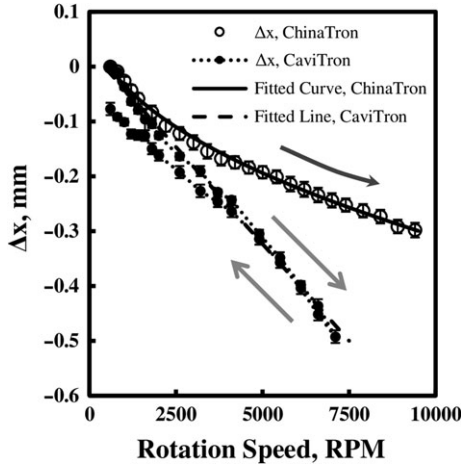

Figure 3. Meniscus displacement from initial position of constant-volume water in the CaviTron (closed circles) and in ChinaTron (opened circles). Δ*x* was the meniscus displacement at a specific RPM from its initial position (at 600 RPM). Error bars were standard errors of $N = 8$ repeats. Gray arrows indicated the direction of rotation speed changed. CaviTron and ChinaTron specify different centrifuge systems as described in the Materials and methods.

However, the movement of menisci from 600 RPM to 9400 RPM reached 0.533 mm, while the meniscus should move only 10 μm if evaporation was the only cause of the meniscus movement.

In Figure 3 the meniscus position changed after the RPM was increased then decreased. The non-linear relationship might be a consequence of the evaporation rate changing as a function of RPM. Equations (5) and (6) gave the best fit relationships shown in Figure 3, and these equations were used to correct water extraction curves; the corrections amounted to ~15% of the extraction volume. We chose a linear empirical function for results obtained in the CaviTron centrifuge but preferred a power function for the correction of data obtained in the ChinaTron centrifuge. Both fitted functions gave similar *r*-squared values (R^2 = 0.994 and 0.996).

$$X_{\text{cal,CaviTron}} = (-7.07 \times 10^{-5}) \times \text{RPM} + 3.00 \times 10^{-2}(\text{mm}) \quad (5)$$

$$X_{\text{cal,ChinaTron}} = (-5.98 \times 10^{-3}) \times \text{RPM}^{0.46} + 0.112(\text{mm}) \quad (6)$$

Water extraction curves in Robinia *segments*

In Figure 4 all curves are scaled to the volume of the stem, and different combinations of treatments are shown. The most dramatic comparison between examples are between 'bark removed' and 'painted'. In the latter case, the wet sapwood was painted with nail polish to prevent evaporation. The mean curve for the painted stems was significantly higher than that of the bark removed curve for all tensions. For the painted case, the volume of water extracted was 7.0% of the stem volume, which was more than twice the value as in the bark removed case. In contrast, the difference in extraction volume with bark present was not significantly different whether the stems were flushed or not flushed before the extraction curve was obtained. The values in Figure 5, focused on the volume of water extraction from the stems in the second Weibull curve, where the curves for flushed, unflushed and painted were not significantly different. However, the bark removed case was significantly different from all the other curves.

Towards the end of our experiments, we tested the water extraction system using a digital camera that automatically recorded the volume extraction. The results in Figure 6 were for one set of results on only one sample but were typical of many experiments. At each tension, the water extraction curves reach a peak followed by a volume loss that must be caused by evaporation of water from the water surface in the cuvettes and/or from the stems surfaces.

All the water extraction curves (except for the bark removed cases) were also combined and computed as percentage loss of volume (PLV) after subtraction of the first Weibull curves (Figure 7). The mean PLV curve showed an s-shaped (or sigmoid) curve, and the T_{50} was 4.56 ± 0.08 MPa, which was 0.7 MPa higher than that of bench dehydration curve.

Visualization of spin-induced embolisms

Staining experiments were done on replicate stems flushed but not centrifuged (0 MPa treatment) and centrifuged to tensions of 1, 2, 3, 4, 5 MPa ($N = 4$ each). Stem segments were harvested near the axis of rotation where tension was highest. The theoretical PLCs (PLC_{stain}s) at the tension of 1 MPa and 2 MPa were 27.1 ± 3.1% and 27.3 ± 1.2% (Figure 7, hollow diamonds, $N = 20$ combined data), respectively, and had insignificant difference from each other ($P > 0.01$). Then PLC_{stain}

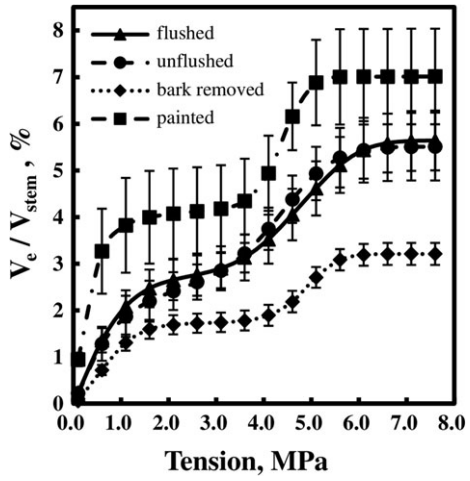

Figure 4. Water extraction curves were scaled to stem volume, V_e was the cumulative volume extracted water and V_{stem} was the stem volume. Bark removed means the bark was removed from the sapwood and the wet sapwood was left exposed to the air. Painted means the bark was removed but the wet sapwood was sealed with nail polish to reduce evaporation. Flushed and unflushed means the stems were flushed with 0.01 KCl to remove native embolisms or not, respectively. Error bars as ± SE.

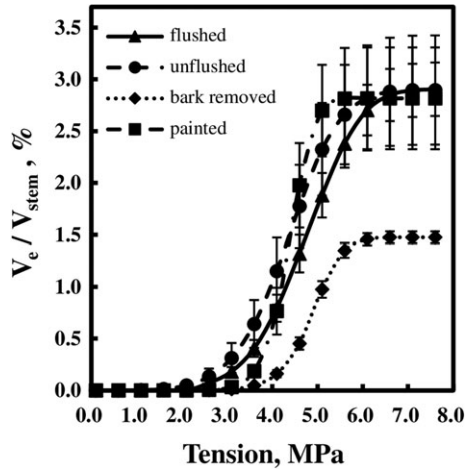

Figure 5. Water extraction curves derived from Figure 4 by subtraction of the first Weibull curve from the second.

significantly increased from 46.6 ± 3.7% at 3 MPa to 62.2 ± 2.6% at 4 MPa, and finally reached 94.1 ± 0.9% at 5 MPa. Suppose that the PLC_{stain} at 1 MPa was the background value, the corrected PLC_{stain}s were obtained by 100 × ($PLC_{stain,T}$ − $PLC_{stain,1\ MPa}$)/(100 − $PLC_{stain,1\ MPa}$) and were used to plot the relationship between PLCs vs induced tensions. This was done because this species frequently had tyloses visible in vessels. Tyloses normally grow in vessels that have been embolized for a long time (Tyree and Zimmermann 2002).

We suggested that the increase of unstained vessel ought to be related to the induced tension in the middle of the stem segment, and hence, a plot of VC in terms of the stain visualization, namely, a stain curve, as a function of tension is shown in Figure 7. The stain curve displayed an s-shaped Weibull distribution, in which T_{50} was 3.89 MPa.

Discussion

The four-cuvette system separated the injection cuvette and the flow-driven cuvette, and the effervescence was therefore effectively suppressed in the stem-hosting reservoir during the water injection. The vulnerability curves measured by the newly designed four-cuvette rotor system showed less vulnerable resistance to cavitation (Figure 2), but this new rotor technique did not remove the recalcitrant VC. Wang et al. (2014*a*) found that the K_h of *Robinia* stem could decrease by 80% during the 4-h K_h measurement at a constant low rotational speed. This finding indicated that the induced flow of degassed solution seeded cavitation partly because water injection inevitably introduced bubbles. More recently, an investigation of the influence of flushing on VC shape indicated that static vacuum infiltration could introduce micro-bubbles and result in cavitation (Pivovaroff et al. 2016). Though the four-cuvette system isolates macro-bubbles from entering the flow-driven cuvette, it is less possible to eliminate micro-/nano-bubbles from the solution. In addition, it is not certain if there is a different source of hypothetical nanoparticles seeding premature embolism; the particles may arise from the cut surface of the stem or may already be present in the injected water. There are cut-open living cells at the surface of any cut stem, and if these cells are quite long then the cell contents would not quickly fall out; however, osmosis would slowly push living cell contents from the cut-open cells into the cuvettes that could then be sucked into vessels and seed cavitation during traditional measurements of K_h in a ChinaTron. However, when water extraction curves are done, these living cell contents (organelles and membrane fragments) will be pushed away from vessels.

In the process of calibrating for menisci position, the difference of water weight in cuvettes was less than 0.001 g, before and after spinning from 600 to 9400 RPM. If the menisci position were only affected by this minor change of weight, then the meniscus position would only change by 0.010 mm. However, the movement of menisci caused by increasing the RPM from 600 to 9400 RPM equaled 0.533 mm, which was 53 times the position displacement caused by water loss. Since both menisci did move eccentrically from the rotating axis, the large displacement with increasing RPM was probably caused by the elastic deformation of the cuvettes and rotor under the centrifugal forces induced by spinning. Therefore, any studies on water extraction curves by different instruments or cuvette types should be corrected by experiments such as those in Figure 3 that measured cuvette/rotor deformation.

In the original Bordeaux extraction method (Pivovaroff et al. 2016), all the extraction curves were scaled to the maximum

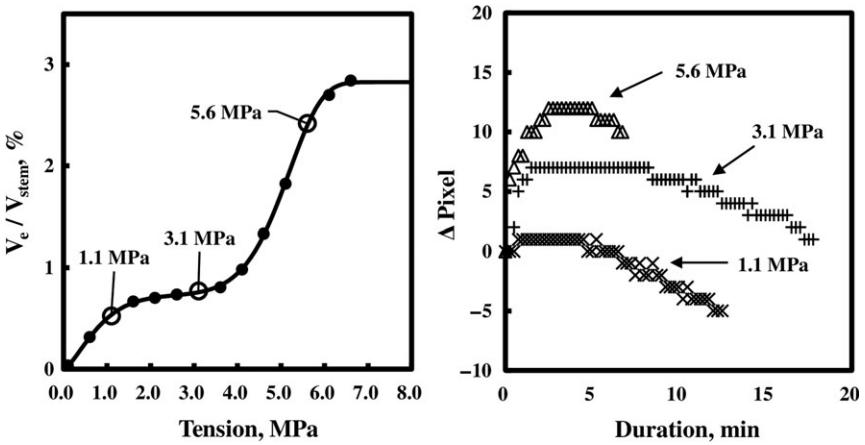

Figure 6. A typical water extraction curve measured on a single stem segment (left) and the raw data of the tempo of water extraction volume (right). One pixel is equal to ~1.745 mm^3 of water extraction volume.

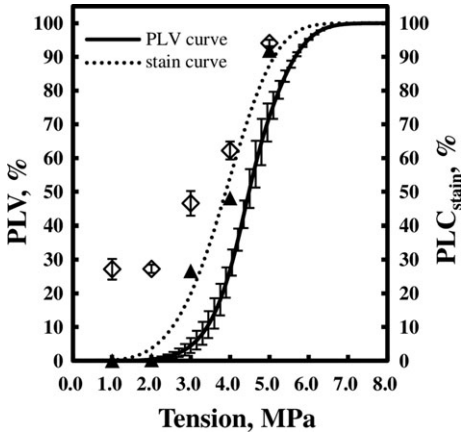

Figure 7. The mean water extraction curves computed as percentage loss of volume (PLV) after subtracting the first Weibull curves (solid line) and the curve measured by the stain method in *Robinia* (dotted line). The mean PLV curve was the combinations of flushed, unflushed and painted cases, since there were no significant differences between each other. In the stain curve, hollow diamonds with error bars ($N = 4$) represent for PLC_{stain}s, % (calculated by Eq. (4)) at given tensions, and solid triangles represent for the corrected PLC_{stain}s, % since 27.1 ± 3.1% of PLC_{stain} at 1 MPa was mainly derived from vessel conduits previously embolized due to tyloses. The T_{50}s of stain curve and PLV curve were 3.89 MPa and 4.56 ± 0.08 MPa, respectively.

volume extracted, V_{max}, and bark was removed to eliminate water extraction from bark without proof that much water is extracted from bark and without proof that other problems were not introduced by bark removal. In our studies, the results in Figure 6 gave examples about how the Bordeaux extraction methods probably need improvement. From these curves, it occurred to us that water extraction and evaporation occurred simultaneously, and the peak value was not a true peak but was the volume lost up until the time at which the rate of water extraction equaled the rate of evaporation. Beyond the time of the peak extraction, the water extraction rate gradually fell to zero, and the plot of the meniscus position vs time might reach a constant slope from which the evaporation rate could be evaluated. In addition, it always occurred that the volume of the extracted water decreased at high rotational speeds due to severe evaporation in our measurements on barkless *Robinia* stems. In the future, we think it may be possible to compute the true volume of water extraction from a more complete knowledge of how evaporation changes during the experiments. For example, if some of the water evaporates from water in the cuvettes, the rate of evaporation might increase as a function of RPM; this dynamic exists because rotational speed causes an increased air flow velocity relative to the frame of reference of the rotating water, thereby reducing the boundary layer thickness over the water and near the stems and causing an increase of the evaporation rate.

Contrary to Pivovaroff's assumption (Pivovaroff et al. 2016) that the extracted water at low tension could come from bark, the bark removal followed by nail polish painting did not reduce the extracted water at the region of the first Weibull curves. The amount of water extraction observed for the painted case was more than twice the value for the bark removed case (7.0% of the stem volume vs 3.2% of the stem volume, Figure 4). The most likely explanation for finding is that 380 mg of stem water per cm^{-3} (3.8%) of stem volume evaporated in the time that was required to collect the extraction curve. This finding is consistent with the notion that the peak in water extraction (Figure 6) is reduced by the higher evaporation rate of barkless-wet sapwood than from painted sapwood. The increase of extracted water might be due to the idea that vaporization from the surface was reduced by the hydrophobic painting material.

It is interesting that after the subtraction of the first Weibull curves, the second Weibull curves of flushed, unflushed and painted samples became coincident (Figure 5). Together with the evidence in PLV curves (Figure 7), very few xylem conduits lost their water before tension reached 3 MPa. As shown in the staining experiments (Figure 7), the main proportion of

unstained vessels did not experience a fast increase until the xylem tension exceeded 3 MPa, which also agreed with the mid-day xylem tension of 1.5 MPa in *Robinia* stems (Wang et al. 2014*a*). Therefore, the extracted water that contributes to the first Weibull curves is less likely to be coming from vessel lumens than in the second Weibull curve. The water presented in the cut open vessels might be a small fraction accounting for the first part of the Weibull curves (Cochard et al. 2010*b*, Vergeynst et al. 2015), but part of the water was probably released earlier while the stem was spinning in the centrifuge at 600 RPM for balance. In a future study, we could use the 'blowing air' method to empty all the cut open vessels prior to centrifugation to test if this could minimize the first part of the curves. Tyree and Yang (1990) and Vergeynst et al. (2015) postulated that capillary water in the lumens of inactive xylem elements and intracellular spaces could be a possible source responsible for this initial increase in extraction volume at low tension. Furthermore, water released from elastic shrinkage of mainly living cells may contribute to this initial increase of the Weibull curves following the capillary water (Tyree and Yang 1990, Vergeynst et al. 2015, Epila et al. 2017). Pivovaroff et al. (2016) defined 'xylem water extraction curves' to represent the relationship of total extracted water volume with tensions. However, our results suggested that the first Weibull curves should be removed from the water extraction curves to establish an exact 'xylem water extraction curve'. In many species the volume of wood fiber lumens is approximately equal to the volume of vessel lumens; thus, this source of water for the first Weibull deserves more quantitative study.

The difference in T_{50} values between the bench dehydration curve produced from Wang et al. (2014*a*) and the mean PLV curve was 0.70 MPa. However, the difference in T_{50} values between the bench dehydration curve and the mean vulnerability curve measured by the Cochard method was >3 MPa. The close agreement between the extraction curve and the bench dehydration curve gives us confidence that the PLV method might be useful in future. The aim for future studies should be to work out the quantitative relationship between the loss of K_h and loss of water volume from the stems. This will require improved experimental methods in the PLV measurement that somehow corrects for evaporation and will require more careful staining experiments and analysis that allows for comparisons to the PLV and PLC.

The PLV curves measured in this paper were independent of whether the stems were flushed or not. If the nano-particle hypothesis is correct, this means that not enough nano-particles are injected into *Robinia* stems to induce much early cavitation. If all the particles needed to induce cavitation were injected during the flush, then the flushed and unflushed curves should be very different in shape and should have different T_{50} values. In most experimental designs, nano-particles will enter throughout the measuring cycle. In the case of the Cochard rotor, the water flow is measured while the rotor is spinning, and Wang et al. (2014*a*) demonstrated that the amount of water entering is enough to induce an extra increment of PLC after each injection. The Sperry rotor system might be immune to nano-particles because the stem conductivity is measured outside the centrifuge using a conductivity apparatus during which time the stems are under positive pressure; thus, no cavitation can be induced during the measurement of K_h. More work needs to be done to determine if the volume of water injected during conductivity measurements is sufficient to induce more embolism upon the next spin in the Sperry rotor. Tentatively, we assume the measuring cycle of the Sperry rotor to induce embolism followed by a conductivity measurement outside is immune from this problem, but we are not aware of anyone who has proven it is immune to the problem. This should be the focus of future research.

Conclusion

In this paper, first we showed the recalcitrant VCs in *Robinia* could not be eliminated by a redesign of the rotor system. It did not support the hypothesis that the effervescence induced by injection in the traditional Cochard method could be a key factor leading to premature cavitation in vessel conduits. Second, we used the water extraction method to test the hypothesis that the water extraction curves were different from the PLC curves obtained in the typical Cochard CaviTron, which measured water flow through stems while spinning. The dye staining experiments showed that the volume extraction from 0 to 3 MPa in *Robinia* was not related to water loss from vessels, but the second Weibull curve was accompanied by an increase in unstained vessels (=cavitated vessels) of nearly 100%. We had already made some improvements in the Bordeaux method, suggesting that there was no point in removing bark because it would increase evaporation from the entire system, but the observation needs to be tested on more species. Maybe more careful studies in the future could distinguish the water extraction from bark or from other likely sources of water such as ray cells or fiber tracheid cells. The aim is to determine if water extraction from vessels can be related to loss of conductivity in vessels.

Acknowledgments

We thank Lingling Zhang for technical assistance in dye experiments.

Conflict of interest

None declared.

Funding

This work was supported by the Thousand Talent Program sponsored by the Ministry of Education of China to Melvin T. Tyree (Z111021201), the Natural Science Foundation of China project

(No. 31201122) to Guangyuan Du and Fundamental Research Funds of the Central Universities of China (No. 2452015078 to Guangyuan DU and No. 2452015070 to Yan Tang), which were sponsored by the Ministry of Education of China as well.

References

Allen CD, Macalady AK, Chenchouni H et al. (2010) A global overview of drought and heat-induced tree mortality reveals emerging climate change risks for forests. For Ecol Manage 259:660–684.

Allison I, Bindoff N, Bindschadler R et al. (2009) The Copenhagen Diagnosis: updating the world on the latest climate science. The University of New South Wales Climate Research Centre, Sydney, Australia.

Breshears DD, Cobb NS, Richd PM et al. (2005) Regional vegetation die-off in response to global change type drought. Proc Nat Acad Sci USA 102:15144–15148.

Choat B (2013) Predicting thresholds of drought-induced mortality in woody plant species. Tree Physiol 33:669–671.

Choat B, Drayton WM, Brodersen C, Mattthews MA, Shackel KA, Wada H, McElrone AJ (2010) Measurement of vulnerability to water stress-induced cavitation in grapevine: a comparison of four techniques applied to a long-vesseled species. Plant Cell Environ 33:1502–1512.

Cochard H (2002) A technique for measuring xylem hydraulic conductance under high negative pressures. Plant Cell Environ 25:815–819.

Cochard H, Herbette S, Hernández E, Hölttä T, Mencuccini M (2010*a*) The effects of sap ionic composition on xylem vulnerability to cavitation. J Exp Bot 61:275–285.

Cochard H, Herbette S, Barigah T, Badel E, Ennajeh M, Vilagrosa A (2010*b*) Does sample length influence the shape of xylem embolism vulnerability curves? A test with the Cavitron spinning technique. Plant Cell Environ 33:1543–1552.

Cochard H, Badel E, Herbette S, Delzon S, Choat B, Jansen S (2013) Methods for measuring plant vulnerability to cavitation: a critical review. J Exp Bot 64:4779–4791.

Epila J, De Baerdemaeker NJ, Vergeynst LL, Maes WH, Beeckman H, Steppe K (2017) Capacitive water release and internal leaf water relocation delay drought-induced cavitation in African *Maesopsis eminii*. Tree Physiol 37:481–490.

Feng F, Ding F, Tyree MT (2015) Investigations concerning cavitation and frost fatigue in clonal 84K poplar using high-resolution cavitron measurements. Plant Physiol 168:144–155.

Martin-StPaul NK, Longepierre D, Huc R, Delzon S, Burlett R, Joffre R, Rambal S, Cochard H (2014) How reliable are methods to assess xylem vulnerability to cavitation The issue of 'open vessel' artifact in oaks. Tree Physiol 34:894–905.

McDowell N, Pockman WT, Allen CD et al. (2008) Mechanisms of plant survival and mortality during drought: why do some plants survive while others succumb to drought? New Phytol 178: 719–739.

Pivovaroff AL, Burlett R, Lavigne B, Cochard H, Santiago LS, Delzon S (2016) Testing the 'microbubble effect' using the Cavitron technique to measure xylem water extraction curves. AoB Plants 8:1–10.

Tyree MT, Sperry JS (1989) Vulnerability of xylem to cavitation and embolism. Annu Rev Plant Physiol Plant Mol Biol 40:19–30.

Tyree MT, Yang S (1990) Water-storage capacity of *Thuja*, *Tsuga* and *Acer* stems measured by dehydration isotherms. Planta 182:420–426.

Tyree MT, Zimmermann MH (2002) Xylem structure and the ascent of sap, 2nd edn. Springer, Berlin, Germany.

Vergeynst LL, Dierick M, Bogaerts JAN, Cnudde V, Steppe K (2015) Cavitation: a blessing in disguise? New method to establish vulnerability curves and assess hydraulic capacitance of woody tissues. Tree Physiol 35:400–409.

Wang R, Zhang L, Zhang S, Cai J, Tyree MT (2014*a*) Water relations of *Robinia pseudoacacia* L.: do vessels cavitate and refill diurnally or are R-shaped curves invalid in *Robinia*? Plant Cell Environ 37: 2667–2678.

Wang YJ, Burlett R, Feng F, Tyree MT (2014*b*) Improved precision of hydraulic conductance measurements using a Cochard rotor in two different centrifuges. J Plant Hydraul 1:0007e.